ARTICLE   OPEN

Edge mode percolation and equilibration in the topological insulator cadmium arsenide

Simon Munyan [1], Binghao Guo [1], William Huynh[1], Victor Huang[1] and Susanne Stemmer [1] ✉

Two-dimensional topological insulators can feature one-dimensional charge transport via edge modes, which offer a rich ground for studying exotic quasi-particles and for quantum materials applications. In this work, we use lateral junction devices, defined by nanoscale finger gates, to study edge mode transport in the two-dimensional topological insulator Cd_3As_2. The finger gate can be tuned to transmit an integer number of quantum Hall edge modes and exhibits full equilibration in the bipolar regime. When the Fermi level of the channel crosses a Landau level, reflected modes percolate through the channel, resulting in an anomalous conductance peak. The device does not fully pinch off when the channel is tuned into the topological gap, which is a sign of remnant modes in the channel. These modes are expected from band inversion, while residual bulk conduction associated with the disorder potential may also play a role.

INTRODUCTION

Lateral junctions are a useful tool for manipulating and studying topological edge modes. In quantum Hall samples, these junctions have enabled an understanding of equilibration amongst chiral edge states in the unipolar and bipolar regimes[1–9]. Thus far, studies of lateral junctions have been mostly limited to topologically trivial materials in the quantum Hall regime, such as GaAs/AlGaAs quantum wells[1,2,8] and graphene[4–7]. Two-dimensional topological insulators are an exciting material platform for lateral junctions, as they provide an opportunity for probing both the helical edge modes of the quantum spin Hall (QSH) effect and the chiral edge modes of the quantum Hall effect[10]. One hurdle is that helical edge modes are extremely sensitive to disorder and reports of their quantized conductance remain limited to short channel devices[11–13]. A lateral junction defined by a short finger gate addresses this issue by requiring the QSH modes to be coherent only across the nanoscale channel. QSH edge modes are protected by time-reversal symmetry and their behavior in finite magnetic fields is not fully understood[14–19]. Lateral junctions can reveal how edge modes interact with a finite magnetic field and with disorder, which will allow for improved design and material considerations for more exotic experiments aimed at studying quantum interference, Majorana bound states, and interactions[20–23].

Epitaxial thin films of cadmium arsenide (Cd_3As_2) are a platform for studying edge- mode transport in a topological material. For a range of film thickness, (001) Cd_3As_2 hosts a two-dimensional topological insulator (2D TI) state[24] characterized by a pair of crossing zeroth Landau levels and a zero field topological gap[25]. Helical edge modes arising from the quantum spin Hall effect are expected to exist when the Fermi level is tuned into this gap[24]. The topological gap persists to a finite magnetic field until the zeroth Landau levels cross and a trivial gap reopens[25]. Like graphene, Cd_3As_2 features electron- and hole-like Landau levels which are accessible with magnetic field and gate voltage, allowing for studies of equilibration in the bipolar regime of a lateral junction. Furthermore, spin degeneracy is fully lifted with

the onset of Landau quantization, and individual edge modes are clearly distinguished for a wide range of filling factors.

In this work, we report on a lateral junction device fabricated on a 2D TI Cd_3As_2 thin film. The finger gate controllably transmits individual chiral edge modes in the unipolar regime. As the channel is tuned through a Landau level, we observe the reflected modes partially transmitting through the channel before being fully reflected once again. We also examine the device with the channel tuned into the trivial and topological gap. We observe complete pinch-off when tuned into the trivial gap, but a remnant conductance in the topological gap. We discuss the roles of disorder and magnetic fields to explain our observations.

RESULTS

Landau level spectrum of the 2D TI Cd_3As_2 thin film

Figure 1a shows the device and measurement geometry for the lateral junctions (see also Supplementary Fig. 1). The diagonal conductance was calculated using the additivity of voltages as $G_D = I/(|V_H| + V_L)$. Before we discuss the results from the lateral junctions, we show in Fig. 1b the longitudinal conductivity as a function of an out-of-plane magnetic field and gate voltage at 2 K on a Hall bar without a finger gate. The Hall bar was fabricated from the same sample with an 19 nm Cd_3As_2 film to serve as a reference device. The crossing of two zeroth Landau levels at $B_c \approx$ 7 T and $V_g \approx -2$ V is a hallmark of the 2D TI (for a detailed discussion see ref. [25]). Around charge neutrality, which we take to be the resistance maximum of the $v = 0$ state, this crossing separates a topologically non-trivial gap ($B < B_c$) from a trivial gap ($B > B_c$). Helical edge modes are expected to exist when the Fermi level resides in the non-trivial gap, though they are no longer protected by time reversal symmetry. Additional Landau levels originating from a higher-energy subband appear at $V_g \sim 2$ V[25]. Figure 1c shows the Hall conductivity at three magnetic fields below, near, and above B_c, respectively. Both even and odd integer plateaus are seen in the Hall conductivity, indicating fully lifted spin degeneracy, as expected for a 2D TI[15]. Furthermore, a

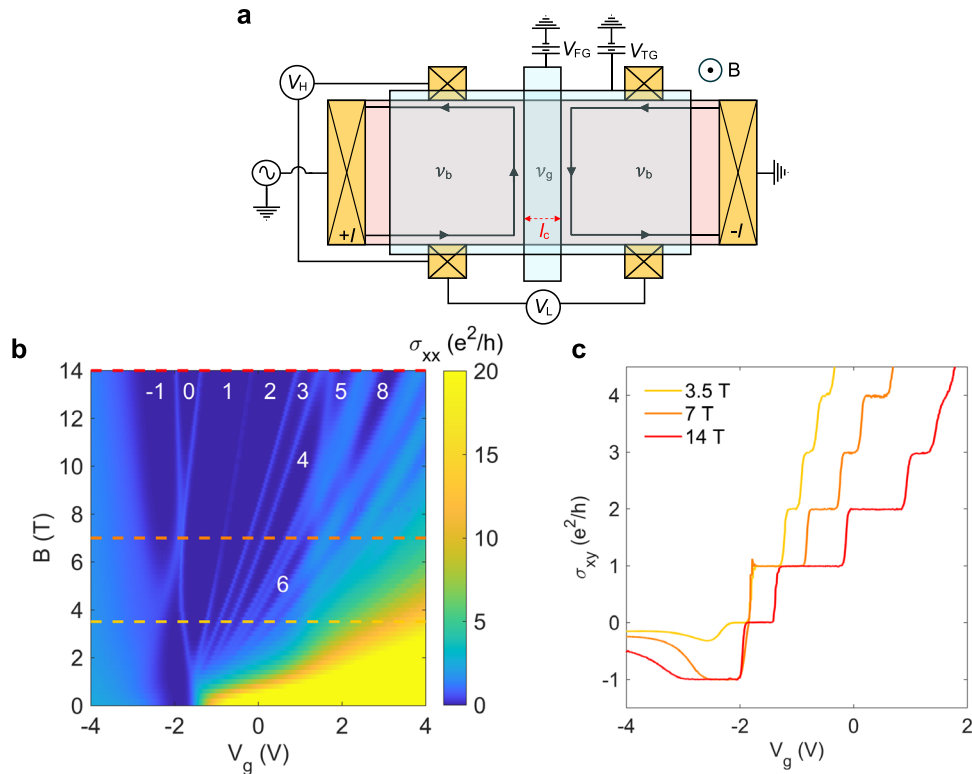[1]Materials Department, University of California, Santa Barbara, CA 93106-5050, USA. ✉email: stemmer@mrl.ucsb.edu

Fig. 1 Device schematic and Landau level spectrum. a Lateral junction device schematic and contact configuration. **b** Longitudinal conductivity measured using a Hall bar as a function of magnetic field and gate voltage at 2 K. Colored dashed lines indicate the three magnetic fields of the detailed studies of the lateral junctions. **c** Hall conductivity as a function of gate voltage at the select magnetic fields at 2 K.

$\nu = 0$ plateau signifies the non-trivial and trivial gaps in the 3.5 T and 14 T traces, respectively.

Edge mode transmission and equilibration

We begin by examining a lateral junction device with a channel length $l_c = 500$ nm at $B_c \approx 7$ T. At this field, the zeroth Landau levels cross and no $\nu = 0$ plateau exists [see Fig. 1b, c]. Figure 2a shows traces at different ν_b as V_{FG} is varied. For each trace, a plateau is observed at $G_D \approx \nu_b e^2/h$ when $\nu_g = \nu_b$, which corresponds to full transmission of all available edge modes. As V_{FG} is decreased so that $\nu_g < \nu_b$, the conductance decreases monotonically to the next plateau, indicating the reflection of one edge mode and transmission of the remaining $\nu_b - 1$ modes [see Fig. 2b for the case of $\nu_b = 2$ and $\nu_g = 1$]. Upon further decreasing V_{FG}, peaks are observed in the conductance along the edges of the plateaus before transitioning to the next, lower plateau. These peaks suggest partial transmission of reflected edge modes and will be discussed in depth later. Upon further decreasing V_{FG} to $\nu_g = -1$, the conductance decreases to a finite minimum rather than to zero. These minima arise from equilibration between electron-like modes in the bulk and a hole-like mode in the channel [Fig. 2c]. Equilibration allows for charge transfer between the edge modes and yields a finite conductance through the channel. Theoretical values of the conductance from a simple model following Landauer-Büttiker theory are shown by color-coded dashed lines in Fig. 2a and show good agreement with the data (see Supplementary Table I for the calculated values). Further agreement is seen in the other bipolar case, where $\nu_b = -1$ and $\nu_g \geq 0$ (Supplementary Fig. 2). As discussed in a prior work, no spin-selectivity is seen in the equilibration[26]. In contrast, for positive V_{FG}, when $\nu_g > \nu_b$, we observe a fluctuating and step-wise decreasing conductance. This decrease arises from equilibration

between accumulated electron-like modes in the channel and the transmitted modes from the bulk [Fig. 2d][6,26]. The expected plateaus are not well-defined, possibly owing to the short channel length. Past works on GaAs/AlGaAs quantum wells have estimated the equilibration length to be on the order of 10–100 μm, which would explain the incomplete degree of equilibration[27]. We leave more detailed discussions for future work.

We now consider the role of the magnetic field on the peaks (Fig. 3). At 14 T [Fig. 3a], the peaks on the edges of the plateaus are strongly suppressed compared to the 7 T data shown in Fig. 2a. We now also see well quantized plateaus for $\nu_g = -1$ due to equilibration. Since equilibration occurs between edge states at the finger gate boundary via inter-Landau-level transitions, it is clear that this type of transition is not significantly suppressed at high field. At lower magnetic fields [3.5 T, see Fig. 3c], the peaks on the plateau edges are even larger than at 7 T, to the point that some plateaus are lost.

Channel pinch-off in trivial and topological regimes

When the channel is tuned into the gap, clear differences exist in G_D between the topological gap (low fields) and the trivial gap (high fields). At 14 T, when the finger gate is tuned to $\nu_g = 0$, the conductance drops to $G_D < 0.1 e^2/h$, signaling a complete pinch-off of the channel [Fig. 3a]. This is expected, as a trivial gap exists at 14 T in the Cd_3As_2 thin film without any edge modes [Fig. 3b]. In contrast, at 3.5 T [Fig. 3c], a non-trivial gap exists, which is expected to host a pair of counter-propagating edge modes originating from band inversion (the edge states may scatter and gap out due to time-reversal symmetry breaking[16,19]) [Fig. 3d]. Interestingly, in the non-trivial gap, when the finger gate is tuned to $\nu_g = 0$, the conductance decreases only to a finite minimum
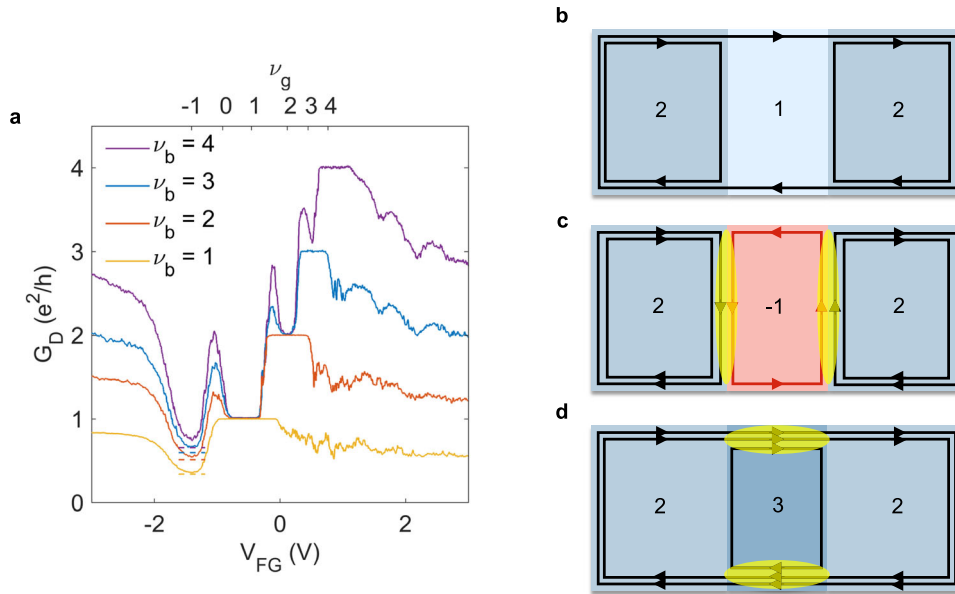
Fig. 2 Edge mode transmission and equilibration. a Diagonal conductance of a 500 nm channel lateral junction device at 7 T and 12 mK. **b** Edge state picture for the case of partial transmission ($v_b = 2$, $v_g = 1$). **c** Edge state picture for the bipolar regime ($v_b = 2$, $v_g = -1$). Yellow regions indicate equilibration between modes. **d** Edge state picture for the accumulation regime ($v_b = 2$, $v_g = 3$).
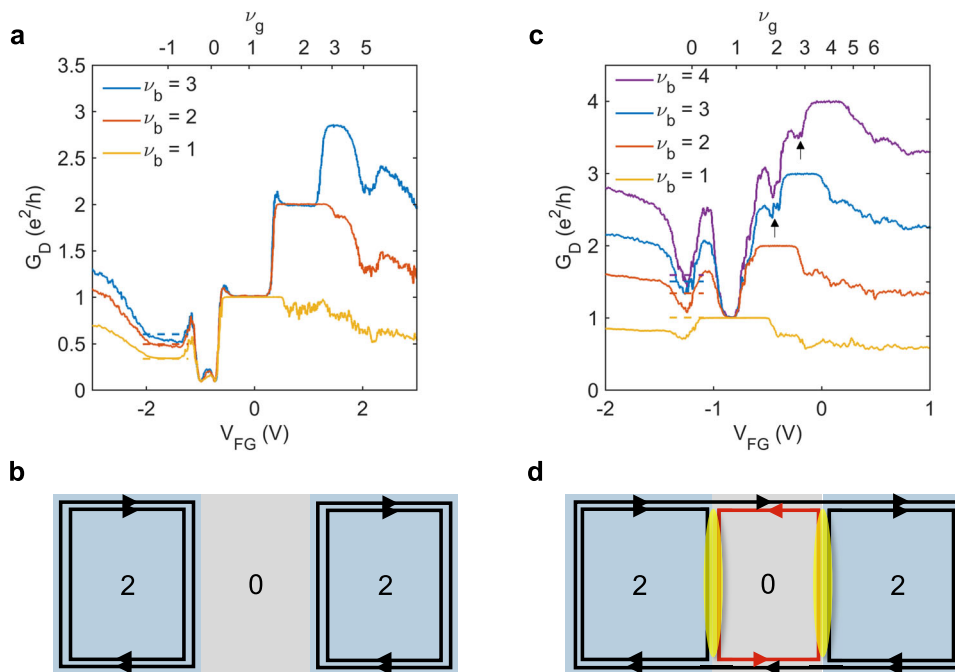

Fig. 3 Channel pinch-off in trivial and topological regimes. a Diagonal conductance of a 500 nm channel lateral junction device at 14 T and 12 mK. **b** Edge state picture for $v_g = 0$ at 14 T. **c** Diagonal conductance of a 500 nm channel lateral junction device at 3.5 T and 12 mK. Black arrows indicate plateaus which are obscured by the peaks. **d** Edge state picture for $v_g = 0$ at 3.5 T. Equilibration is indicated in yellow at the finger gate boundary.

value. This minimum G_D value increases systematically with v_b and also decreases with channel length (see Supplementary Fig. 3).

DISCUSSION
We next discuss the data, beginning with the conductance peaks seen on the edges of the plateaus. These peaks appear only for plateau transitions where $v_b - v_g \geq 1$, such that at least one of

the modes from the bulk is already completely reflected. Furthermore, the peaks are strictly higher in conductance than the underlying plateau but lower than the highest plateau. Both of these facts point to the peaks originating from the $v_b - v_g$ reflected modes leaking through the channel and contributing an additional conductance to the already perfectly transmitted v_g edge modes. These peaks can be explained with a model[1,2] that involves percolation through the channel via localized states
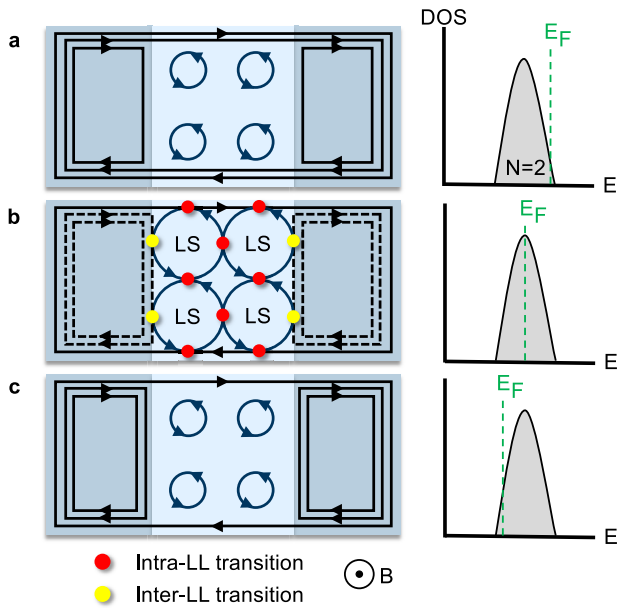
Fig. 4 **Edge mode percolation via localized states.** Schematic of percolation through localized states in the channel for $v_b = 3$ when the Fermi level E_F is tuned through the $N = 2$ Landau level. **a** For $v_g = 2$, two edge modes transmit through the channel and one is completely reflected. **b** The Fermi level passes through the center of the $N = 2$ Landau level and the classical orbits of the localized states grow, facilitating partial transmission of the reflected modes. **c** The Fermi level is further reduced such that $v_g = 1$ and two edge modes are completely reflected.

in the tails of Landau levels [see Fig. 4 for a schematic where $v_b = 3$]. When $v_g \approx 2$ and the Fermi level is in the high energy tail of a disordered Landau level, the semiclassical orbits of the localized states are small and one mode is completely reflected without percolation [Fig. 4a]. As the Fermi level in the channel approaches the center of a Landau level, the orbits of the localized states grow, and come into close proximity with the extended edge states at the finger gate boundary [Fig. 4b]. Consequently, charge transfer can then occur between the reflected edge modes from the bulk and localized states at the finger gate edge in a two-step process. First, charge tunnels between the reflected modes and the localized state at the gate edge through inter-Landau-level transitions. Second, this charge percolates through the channel by tunneling between localized states via intra-Landau-level transitions[28]. This charge transfer pathway has been established in theory[2] and observed experimentally with scanning tunneling spectroscopy[29]. As the Fermi level is further reduced to $v_g \approx 1$, the localized states shrink and two modes are completely reflected.

This model explains a number of patterns in our data, which are related to the inter- and intra-Landau-level transitions, respectively. For one, the model explains why no peaks are seen for the transition from $v_g = v_b$ to $v_g = v_b - 1$ [see Fig. 2a]. In this case, there are no modes which are completely reflected, so decreasing V_{FG} results in a monotonic decrease of the conductance as one edge mode is gradually pinched off. On the other hand, for $v_b - v_g \geq 1$, there is at least one fully reflected mode which can percolate through the channel when the Fermi level passes through a Landau level, giving rise to a peak in conductance between subsequent plateaus. The conductance peaks increase in amplitude as v_g decreases, owing to the increasing number of reflected modes ($v_b - v_g$) which are available to tunnel into the localized states of the channel via inter-Landau-level transitions. The amplitude also increases with

v_b for the same v_g, which is also explained by the increasing number of reflected modes. In both these cases, an increase in the number of inter-Landau-level transitions between reflected modes and localized states at the finger gate edge is responsible for the increase in conductance peaks. A comparison of devices with different channel lengths shows that the peaks decrease in amplitude for longer channels, in agreement with past studies (Supplementary Fig. 4)[2]. The channel length is directly related to the number of intra-Landau-level transitions that must occur between localized states for the charge to percolate through the channel. Given that the probability of a single intra-Landau-level transition is less than unity, the total probability of percolation naturally decreases with the channel length, as more transitions are required to span the channel[27]. Therefore, percolation is suppressed through longer channels.

The fact that the peaks are diminished at 14 T shows that the intra-Landau-level transitions are suppressed by larger magnetic fields, which shrink the classical orbits of the localized states, reducing the probability of transitions between them [Fig. 3a]. This picture is borne out by the more prominent peaks at lower magnetic fields [Fig. 3c]. The data also show that inter-Landau-level transitions are not significantly suppressed at high field, because we see well-quantized plateaus for $v_g = -1$ due to equilibration. Since equilibration occurs between reflected electron-like edge modes and a hole-like edge mode at the finger gate boundary via inter-Landau-level transitions, it is clear that this type of transition is not significantly suppressed at high field.

We next discuss the nature of the states that allow for the observed transmission when the channel is tuned into the nontrivial gap at $B < B_c$ [Fig. 3c]. As shown in Fig. 3d, in the nontrivial gap, one of the modes belonging to the pair of helical edge states in the channel matches with the $v = 1$ mode from the bulk, facilitating transmission. The other mode in the channel equilibrates with reflected modes from the bulk, contributing to a fractional conductance[30]. This matching is possible because the $v = 1$ mode in the bulk region originates from the same Landau level as the clockwise-propagating spin-up mode in the topological gap[19]. Furthermore, at a finite magnetic field, the edge modes are spatially separated according to the picture drawn in Fig. 3d[10]. Theoretical conductances for this scenario are indicated by dashed lines in Fig. 3c. Consistent with the experiment, the calculated conductance minimum increases with v_b. The actual values are, however, systematically lower than the theoretical values. This may be in part due to the finite magnetic field, which breaks time-reversal symmetry and lifts the protection from backscattering. Alternatively, we expect that the disorder potentially implicated in our previous discussion also plays a role when $v_g = 0$. It is well known that in small gap semiconductors, disorder gives rise to "charge puddles" in the gap around charge neutrality[31,32]. These puddles cause inelastic backscattering of the edge modes and may thus lead to a systematically lower conductance. Both mechanisms may lead to the length dependence of the conductance minimum seen in Fig. S4. However, the deconvolution of these two mechanisms requires future work.

In summary, we have demonstrated controlled transmission of quantum Hall edge modes in a short-channel lateral junction. Anomalous conductance peaks near plateau transitions were explained by percolation through localized states in the channel due to bulk disorder. Magnetic field and channel length dependencies showed that this transmission path is suppressed by reducing intra-Landau-level transitions. In contrast, inter-Landau-level transitions were not significantly affected by magnetic fields. Lastly, we found that the device fully pinches off when the channel is tuned into the trivial gap, but a finite conductance remains when tuned into the non-trivial gap. We attribute this conductance to remnant states in the gap, which

may either be edge states coming from band inversion or localized bulk states due to disorder. Future work will focus on distinguishing these contributions to conductance through variable width devices and non-local resistance measurements.

METHODS

Device fabrication

Lateral junction devices were fabricated from an 19 nm (001) Cd_3As_2 film grown by molecular beam epitaxy on an III–V substrate and buffer layer, as reported elsewhere[25,33]. The film was patterned using electron beam lithography (EBL) to define the device mesa with a width of 10 μm, which was isolated by argon ion milling. Ohmic contacts (Ti/Pt/Au) were patterned with photolithography and deposited by electron beam deposition. A 20 nm-thick Al_2O_3 dielectric layer was deposited via atomic layer deposition at 120 °C. The finger gates (Ni/Au) were patterned using EBL to channel lengths l_c corresponding to 250, 500, or 1000 nm, respectively, and deposited using thermal evaporation. Ti/Pt/Au layers served as Ohmic contacts to the finger gates. A second dielectric layer was deposited to isolate the finger gate from the global top gate. Lastly, the global top gate (Ni/Au) was patterned using photolithography and thermal evaporation. A micrograph of the device is shown in Supplementary Fig. 1.

Measurement

Magnetotransport measurements were performed at 12 mK in a He-3/He-4 dry dilution refrigerator unless noted otherwise. An out-of-plane magnetic field up to 14 T was applied during the measurements. A constant excitation current of 1 nA was sourced at 17.778 Hz between the current contacts. The Hall and longitudinal voltages were measured using lock-in amplifiers. A DC voltage V_{TG} applied to the top gate sets the bulk filling factor v_b, while a voltage V_{FG} applied to the finger gate sets the channel filling factor v_g [Fig. 1a]. The finger gate screens the channel from the influence of the global top gate.

REFERENCES

1. Haug, R. J., MacDonald, A. H., Streda, P. & Klitzing, K. V. Quantized multichannel magnetotransport through a barrier in two dimensions. *Phys. Rev. Lett.* **61**, 2797 (1988).
2. Haug, R. J., Kucera, J., Streda, P. & von Klitzing, K. Scattering experiments in two-dimensional systems in the presence of quantizing magnetic fields. *Phys. Rev. B* **39**, 10892 (1989).
3. Muller, G. et al. Equilibration length of electrons in spin-polarized edge channels. *Phys. Rev. B* **45**, 3932–3935 (1992).
4. Abanin, D. A. & Levitov, L. S. Quantized transport in graphene p-n junctions in a magnetic field. *Science* **317**, 641–643 (2007).
5. Williams, J. R., Dicarlo, L. & Marcus, C. M. Quantum Hall effect in a gate-controlled p-n junction of graphene. *Science* **317**, 638–641 (2007).
6. Özyilmaz, B. et al. Electronic transport and quantum Hall effect in bipolar graphene p−n−p junctions. *Phys. Rev. Lett.* **99**, 166804 (2007).
7. Amet, F., Williams, J. R., Watanabe, K., Taniguchi, T. & Goldhaber-Gordon, D. Selective Equilibration of spin-polarized quantum Hall edge states in graphene. *Phys. Rev. Lett.* **112**, 196601 (2014).
8. Nicoll, G. et al. Spin-selective equilibration among integer quantum Hall edge channels. *Phys. Rev. Lett.* **128**, 056802 (2022).
9. Beenakker C. W. J. & van Houten, H. Quantum transport in semiconductor nanostructures, in: (eds H. Ehrenreich and D. Turnbull) *Semiconductor Hetero-structures and Nanostructures.* Vol. 44, p. 1–228.
10. Calvo, M. R. et al. Interplay of chiral and helical States in a quantum spin Hall insulator lateral junction. *Phys. Rev. Lett.* **119**, 226401 (2017).
11. Konig, M. et al. Quantum spin Hall insulator state in HgTe quantum wells. *Science* **318**, 766–770 (2007).
12. Roth, A. et al. Nonlocal transport in the quantum spin Hall state. *Science* **325**, 294–297 (2009).
13. Wu, S. F. et al. Observation of the quantum spin Hall effect up to 100 kelvin in a monolayer crystal. *Science* **359**, 76–79 (2018).
14. Zhou, B., Lu, H. Z., Chu, R. L., Shen, S. Q. & Niu, Q. Finite size effects on helical edge states in a quantum spin-Hall system. *Phys. Rev. Lett.* **101**, 246807 (2008).
15. König, M. et al. The quantum spin Hall effect: Theory and experiment. *J. Phys. Soc. Jpn* **77**, 031007 (2008).
16. Tkachov, G. & Hankiewicz, E. M. Ballistic quantum spin Hall state and enhanced edge backscattering in strong magnetic fields. *Phys. Rev. Lett.* **104**, 166803 (2010).
17. Maciejko, J., Qi, X. L. & Zhang, S. C. Magnetoconductance of the quantum spin Hall state. *Phys. Rev. B* **82**, 155310 (2010).
18. Chen, J.-C., Wang, J. & Sun, Q.-F. Effect of magnetic field on electron transport in HgTe/CdTe quantum wells: Numerical analysis. *Phys. Rev. B* **85**, 125401 (2012).
19. Scharf, B., Matos-Abiague, A. & Fabian, J. Magnetic properties of HgTe quantum wells. *Phys. Rev. B* **86**, 075418 (2012).
20. Fu, L. & Kane, C. L. Superconducting proximity effect and Majorana fermions at the surface of a topological insulator. *Phys. Rev. Lett.* **100**, 096407 (2008).
21. Li, J., Pan, W., Bernevig, B. A. & Lutchyn, R. M. Detection of Majorana Kramers pairs using a quantum point contact. *Phys. Rev. Lett.* **117**, 046804 (2016).
22. Xue, F. & MacDonald, A. H. Time-reversal symmetry-breaking nematic insulators near quantum spin Hall phase transitions. *Phys. Rev. Lett.* **120**, 186802 (2018).
23. Strunz, J. et al. Interacting topological edge channels. *Nat. Phys.* **16**, 83 (2020). +.
24. Wang, Z. J., Weng, H. M., Wu, Q. S., Dai, X. & Fang, Z. Three-dimensional Dirac semimetal and quantum transport in Cd3As2. *Phys. Rev. B* **88**, 125427 (2013).
25. Lygo, A. C. et al. Two-dimensional topological insulator state in cadmium arsenide thin films. *Phys. Rev. Lett.* **130**, 046201 (2023).
26. Munyan, S., Rashidi, A., Lygo, A. C., Kealhofer, R. & Stemmer, S. Edge channel transmission through a quantum point contact in the two-dimensional topological insulator cadmium arsenide. *Nano Lett.* **23**, 5648–5653 (2023).
27. Haug, R. J. Edge-state transport and its experimental consequences in high magnetic fields. *Semicond. Sci. Technol.* **8**, 131 (1993).
28. Chalker, J. T. & Coddington, P. D. Percolation, quantum tunnelling and the integer Hall effect. *J. Phys. C* **21**, 2665 (1988).
29. Hashimoto, K. et al. Quantum Hall transition in real space: from localized to extended states. *Phys. Rev. Lett.* **101**, 256802 (2008).
30. Gusev, G. M., Levin, A. D., Kvon, Z. D., Mikhailov, N. N. & Dvoretsky, S. A. Quantum Hall effect in n-p-n and n-2D topological insulator-n junctions. *Phys. Rev. Lett.* **110**, 076805 (2013).
31. Väyrynen, J. I., Goldstein, M. & Glazman, L. I. Helical edge resistance introduced by charge puddles. *Phys. Rev. Lett.* **110**, 216402 (2013).
32. König, M. et al. Spatially resolved study of backscattering in the quantum spin Hall state. *Phys. Rev. X* **3**, 021003 (2013).
33. Goyal, M. et al. Carrier mobilities of (001) cadmium arsenide films. *APL Mater.* **8**, 051106 (2020).

AUTHOR CONTRIBUTIONS

S.M. designed the device and experiment, fabricated the lateral junction devices, performed all measurements, and analyzed the data. B.G. and V.H. grew the film. W.H. fabricated and measured the Hall bar device. S.M. and S.S. prepared the paper and all authors commented on it.

COMPETING INTERESTS

The authors declare no competing interests.

ADDITIONAL INFORMATION

Supplementary information The online version contains supplementary material available at https://doi.org/10.1038/s41535-023-00602-6.

Correspondence and requests for materials should be addressed to Susanne Stemmer.

Reprints and permission information is available at http://www.nature.com/reprints

Publisher's note Springer Nature remains neutral with regard to jurisdictional claims in published maps and institutional affiliations.